ELSEVIER

Microelectronic Engineering 36 (1997) 125–128

MICROELECTRONIC ENGINEERING

Bohm trajectories for the modeling of tunneling devices

J. Suñé, X. Oriols, J.J. García-García, and F. Martín
Departament d'Enginyeria Electrònica. Universitat Autònoma de Barcelona. 08193-Bellaterra.
Tel. 34-3-581 18 29. Fax. 34-3-581 13 50. e-mail: jsune@cc.uab.es

T. González, J. Mateos, and D. Pardo
Dep. de Física Aplicada. Universidad de Salamanca. 37008-Salamanca. SPAIN.

It is shown that quantum phenomena in electron devices, such as tunneling of electrons, can be modeled using Bohm trajectories. Fowler-Nordheim tunneling in thin-oxide MOS structures and resonant tunneling in double barrier diodes are considered.

1.INTRODUCTION

The tunneling of electrons is of increasing interest in silicon devices. Leakage currents, oxide degradation, dielectric breakdown, hot electron effects, are examples of phenomena which are related to tunneling in MOSFETs. This quantum-mechanical (QM) phenomenon is basic to the operation of devices such as floating gate EEPROMs. Also, new tunneling-based silicon devices are being proposed as alternatives to agressively scaled down MOS transistors [1].

In conventional MOS devices, tunneling has usually been modeled using the WKB approximation. In very thin insulator structures numerical solution of the stationary Schrödinger equation has also been undertaken to reveal aspects which cannot be considered within the former approximation. In general, the results are in quantitative agreement with experiments if one considers the limitations derived from the exponential dependences of the tunneling probability on barrier height and barrier thickness. In the case of tunneling devices such as the resonant tunneling diode (RTD) more accurate simulations have been performed and two main approaches have been considered: the solution of the effective-mass (Schrödinger) equation [2], and the integration of the Liouville equation to obtain the Wigner distribution function [3]. In both cases, self-consistency with the Poisson equation has been accounted for with different degrees of approximation. The first approach assumes full wave-coherence (extended scattering states), and has the severe limitation of using the equilibrium distributions of carriers at the contacts when considering the occupation of these states. The second approach is in principle free of this limitation because scattering interactions can be introduced into the Liouville equation, and the contact distributions are only assumed as boundary conditions. However, the extensive computation burden required by this approach considerably limits the size of the simulation box so that these boundary conditions can be far from being realistic.

A reliable approach for the introduction of tunneling into multidimensional device simulators is still missing. In this regard, the coupling of a QM treatment of tunneling with the semi-classical Monte Carlo (MC) simulation technique would be very convenient because it would allow the simultaneous consideration of scattering and QM coherence effects. For this purpose we are considering two alternatives, i.e. Wigner trajectories [4] and Bohm QM trajectories [5]. In this work we deal with Bohm trajectories in two cases which are interesting for device applications: (1) Fowler-Nordheim (FN) injection in $Si/SiO_2/Si$ structure; and (2) resonant tunneling in double-barrier diodes.

2. BOHM'S INTERPRETATION.

Let us briefly review the basics of Bohm's interpretation for non-relativistic particles [6]. The wavefunction associated to a particle can always be expressed as

$$\psi(x,t) = R(x,t)\exp\left(i\frac{S(x,t)}{\hbar}\right) \qquad (1)$$

with $R(x,t)$ and $S(x,t)$ being real functions. Thus the complex time-dependent Schrödinger equation

PII: S0167-9317(97)00031-2

(TDSE) is found to be equivalent to two real equations: the continuity equation for the presence probability density $P(x,t) = R^2(x,t)$; and another equation which can be interpreted as a modified Hamilton-Jacobi equation. In this scheme, the particle velocity is directly given by $v(x,t) = (1/m)(\partial S(x,t)/\partial x)$, and the classical potential energy $V(x,t)$ is augmented by a new term, $Q(x,t)$, which is interpreted as a quantum potential:

$$Q(x,t) = -\frac{\hbar^2}{2m}\frac{1}{R(x,t)}\frac{\partial^2 R(x,t)}{\partial x^2} \qquad (2)$$

This quantum potential introduces non-local features and modifies the trajectories so that the measurable results of the standard interpretation of Quantum Mechanics are perfectly reproduced. Assuming an initial wavepacket $\Psi(x,0)$, the particle trajectory is causally determined at all instants of time, provided that the initial position x_0 is known. However, because of the limitations of the uncertainty principle, the initial position is not perfectly determined within the initial wavepacket, and the physical quantities must be obtained by averaging over all the possible trajectories weighted by $P(x_0,0)$.

3. NUMERICAL PROCEDURE.

Regarding to the choice of the initial wavefunction, two alternatives have been considered in the literature: stationary scattering states, and localized time-dependent wavepackets. However, since Bohm trajectories associated to the scattering eigenstates of the effective-mass hamiltonian give non-consistent results (this failure is not due to Bohm's interpretation but to the nature of the scattering states themselves), time-dependent wavepackets are required. Our procedure is as follows: (i) we define a gaussian wavepacket located at t=0 in the emitter electrode, far enough from the barriers so that the potential is flat and the probability presence in the barrier region negligible; (ii) we integrate the hamiltonian eigenstates following the method of Vasell et al. [2]; (iii) we project the initial wavefunction onto the obtained basis to calculate $\Psi(x,t)$ by superposition; and (iv) finally we integrate Bohm trajectories. In step (iv), we first calculate R(x,t) and S(x,t) from the wavefunction, we calculate the velocity by dereivation of S(x,t), and we spatially integrate it to obtain the trajectory.

4. RESULTS.

4.1 Fowler-Nordheim tunneling through a thin MOS capacitor.

Consider first a silicon MOS structure with a 4 nm oxide and highly doped electrodes (no band bending effects).

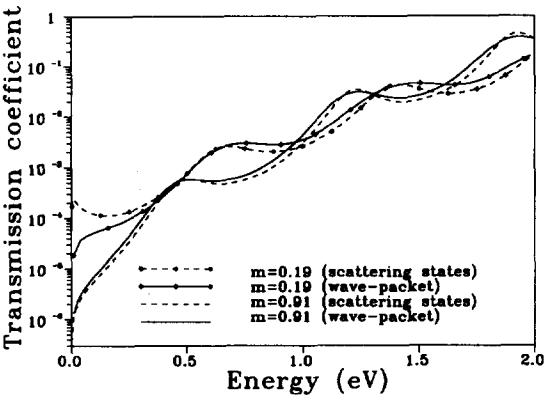

Figure 1. Transmission coefficient for a typical MOS structure with an applied bias of 9 V and oxide thickness of 4 nm in a (100) interface.

In Fig. 1 we show the transmission coefficient as a function of energy for the two sets of silicon valleys ($m^*=0.19m_0$, and $m^*=0.91m_0$) in a (100) interface. We show the results for energy eigenstates and gaussian wavepackets with spatial standard deviation of s_x=7 nm. The results justify this selection of s_x because the transmission coefficient is very similar to that of the scattering eigenstates (spatially more localized packets are too de-localized in energy so that the relevant energy dependences are washed-out). The oscillations are due to reflections at the oxide/anode interface [7] and, as expected, are also apparent in the simulated FN plot (Fig. 2). Since the injection is controlled by the $m^*=0.19m_0$ valley, the following results correspond to this case.

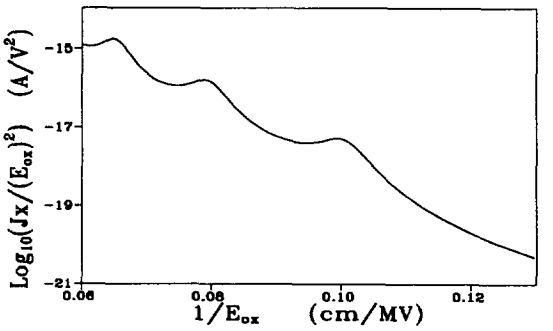

Figure 2. Simulated Fowler-Nordheim plot associated to the structure of fig 1.

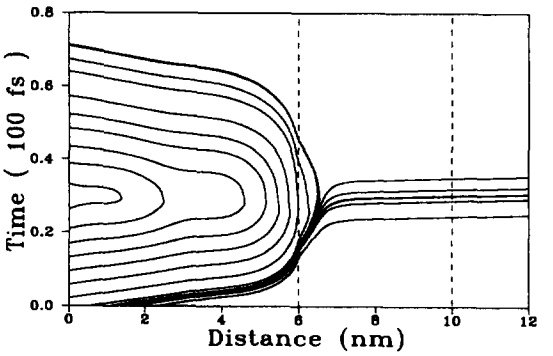

Figure 3. Bohm trajectories for an initial gaussian wave-packet with a central energy of 0.25 eV and a saptial dispersion of 7 nm impinging on the MOS structure (dashed lines) of fig 1.

Fig. 3 shows selected Bohm trajectories for one of the transmission maxima. Most of the trajectories are reflected (without ever reaching the barrier) and only those of the very front of the packet (Bohm trajectories do not cross) are transmitted [8]. No qualitative differences are observed in the trajectories of the transmission minima. The results are consistent because the ensemble of Bohm trajectories perfectly reproduce the evolution of the wavefunction obtained by integration of the time-dependent Schrödinger equation (TDSE). In particular, the transmission coefficient has been calculated by averaging Bohm trajectories with a precision better than 1% in both cases.

4.2 Double barrier resonant tunneling diodes.

RTDs are most adequate to show the strengths of the Bohm's approach because the tunneling phenomenoly is richer than in single barrier structures. Fig. 4 shows Bohm trajectories corresponding to the ground resonance of a double barrier structure typical of AsGa/AsGaAl system. No oscillations are observed and this seems to contradict the usual intuitive interpretation of resonances.

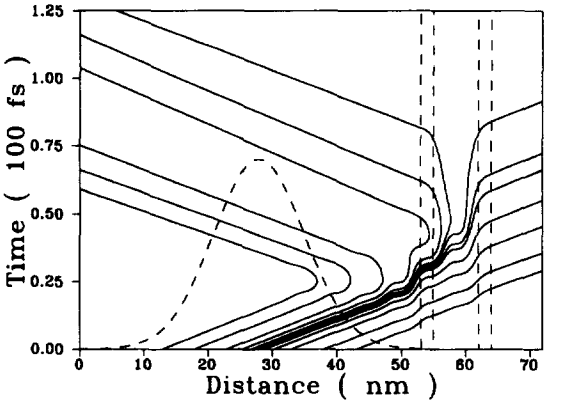

Figure 4. Bohm trajectories associated to an initial gaussian wave-packet (central energy of 0.22 eV and spatial dispersion of 10 nm) incident on a double barrier (dashed lines).

However, the wavefunction solution of the TDSE does not show any oscillation either. This is due to the fact that the local density of states in the well is very narrow. If the well width is increased, the peaks of the density of states become more closely spaced, and the wavefunction shows oscillations.

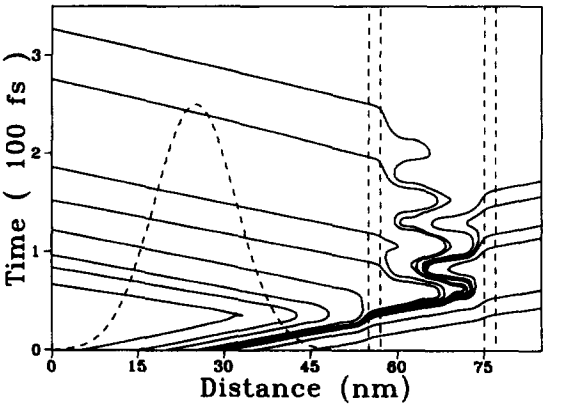

Figure 5. Bohm trajectories associated to an initial gaussian wave-packet (central energy of 0.16 eV and spatial dispersion of 10 nm) impinging on a double barrier (dashed lines) with a wider well.

As expected, Bohm trajectories also bounce between the barriers as shown in Fig. 5 for a 2nm/18nm/2nm structure. The distribution of tunneling times (this quantity is perfectly defined within Bohm's interpretation) also shows periodic bumps according to the sequential attemps to cross the second barrier (Fig. 6) [9].

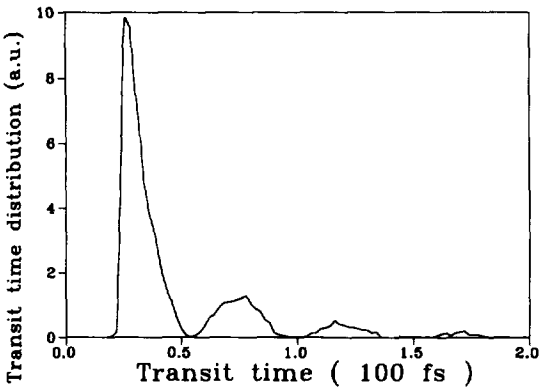

Figure 6. Transit time distribution obtained from 25000 Bohm trajectories for the wave-paket an potential profile of fig 5.

5. Discussion.

We have shown that the tunneling of wavepackets can be described by Bohm trajectories and that, as expected, the obtained results are fully equivalent to those obtained from the wavefunction solution of the TDSE. However, in our opinion, the main interest of this approach is the possibility of using Bohm trajectories for the extension of the MC technique to tunneling devices.

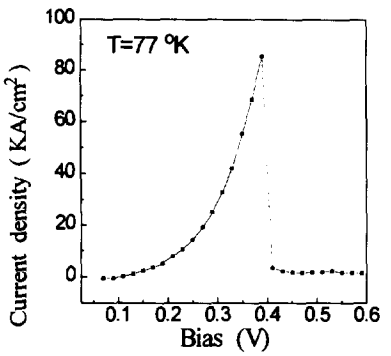

Figure 7. Simulated I-V characteristic of a RTD.

In this regard, we have already developed a preliminary MC simulator (without scattering in the QM region) based on the coupling of classical and Bohm trajectories. The simulator cannot be described here in detail, but we want to show the main results obtained with this tool, i.e. the self-consistent I-V characteristic (Fig. 7); and the position-momentum distribution function at the resonance which clearly shows the tunneling ridge (Fig. 8).

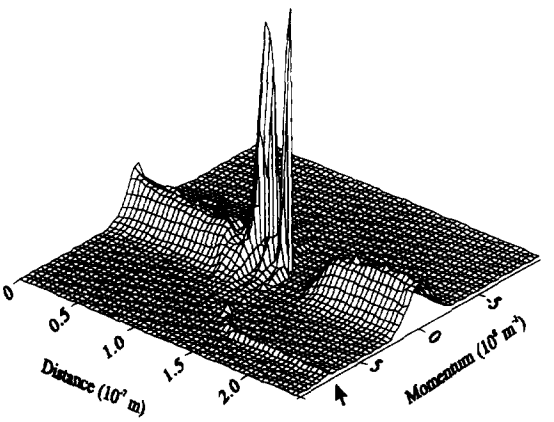

Figure 8. Particle position-distribution function at 0.29 V . Notice the tunneling ridge indicated by an arrow.

These results demonstrate that such simulations are possible and show their great potentiality for the accurate modeling of tunneling in electron devices.

References

1. W.E. Zhang, F.-C. Wang and C.H. Yang, IEEE Trans. Elect. Dev., 43, 1441 (1996).
2. M.O. Vasell, J. Lee, and H.F. Lockwood, J. Appl. Phys., 54, 5206 (1983).
3. W.R. Frensley, Rev. Mod. Phys., 62, 745 (1990).
4. K.L. Jensen and F.A. Buot, IEEE Trans. Elect. Dev., 38, 2337 (1991).
5. C.R. Leavens and G.C. Aers, in: *Scanning Tunneling Microscopy III*, ed. R. Wiesendanger and H.J. Güntherodt (Springer-Varleg, Berlin, 1993) p. 105.
6. D. Bohm, Phys. Rev 85, 166 (1952).
7. J. Maserjian and N. Zamani, J. Appl. Phys., 53, 559 (1982).
8. X. Oriols, F. Martín, and J. Suñé, Phys. Rev. A, 54, 4 (1996).
9. X. Oriols, F. Martín, and J. Suñé, Solid State Comm., 99, 123 (1996).